HIGH RESOLUTION LABORATORY X-RAY TOMOGRAPHY ON ROCKS

E. Rosenberg, P. Guéroult, J. Lynch, M. Bisiaux and R. Ferreira De Paiva
Institut Français du Pétrole, B.P. 311, 92500 Rueil Malmaison

Abstract

Conversion of a standard electron microprobe for use as an X-ray microtomograph is described. Only minor modifications are required, indeed several of the utilities of the microprobe can be used to ensure high resolution radiography and tomography. The impact of the focalized electron beam on a thin film is used to form a " point " X-ray source. This system is capable of 2 micron resolution radiographic imaging. A specimen rotation mechanism allows multiple radiograph acquisition and tomographic reconstruction of the specimen texture. Tomographic resolution depends on the number of acquired radiographs, better than 10 micron resolution in three directions having been demonstrated for 256 x 256 x 256 tomographs reconstructed from 120 radiographs at 3° intervals on small objects. System performance was evaluated by analysis of model and real reservoir rock: glass spheres in a capillary tube, Fontainebleau sandstone and Alwyn sandstone containing quartz, feldpars, and a large amount of kaolinite. Comparison with scanning electron micrographs shows reliable reconstruction of external morphology and helps for identification of minerals. The internal pore structure of the sample and the 3D-distribution of a particular phase can be studied *a posteriori* using the tomography data. Both are useful for the understanding of the macroscopic behavior of the rock in terms of petrophysical properties and wettability.

Introduction

The three dimensional pore structure of reservoir rocks and the wetting of porous media by fluids are of great importance in oil recovery. The transport properties of porous media are determined by their microstructure, i.e. geometry and topology of interconnected pore space. Extraction of petroleum by water injection depends on the displacement of oil in place by water and is also known to be strongly influenced by the wettability of reservoir minerals by water relative to oil [Cuiec, 1991]. On the macroscopic scale several groups have the applied three dimensional imaging possibilities offered by X-ray scanner technology to the study of fluid interactions with reservoir rocks. Tomography using medical scanners does not however reach the spatial resolution necessary for direct visualisation of the pore structure or of the fluids in place. Images produced by medical scanners thus represent weighted average values over the volume elements, or voxels, of the absorption coefficients of the solid, the pore space and any fluids present. Quantitative assessments of porosity and fluid content can only be achieved by subtraction of tomograms before and after fluid injection and only on a scale of the order of a few hundred microns.

Laboratory [Cazaux, 1989, Cheng, 1992] and synchrotron based microscanners [Coles, 1994; Coles ,1996] have recently shown the possibility to image directly in three dimensions the porous structure of real and model porous media. Resolutions below 10 µm have been obtained only by the use of severe collimation of synchrotron radiation [Coles, 1994].

Methods

For the work presented here we use a laboratory microscanner using an electron microprobe as a " point " X-ray source [Ferreira De Paiva, 1996]. This system, based on the original idea of Sasov [Sasov, 1987] and following the development of Cazaux et al.[Cazaux, 1989], is capable of 2 micron resolution radiographic imaging. The basic principle is to use the interaction volume of the focussed electron beam with a thin target as an X-ray source. The object is fixed on a horizontal rotation axis placed between this source and a phosphor screen and a projected image (radiography) is acquired for each angular position of the object. Magnification is changed by varying the position of the target. The projected X-ray micrograph is converted to an equivalent light image by the phosphor screen. The light image is demagnified by a factor of 1.6 onto the CCD via a f1.2 camera objective lens working in macro configuration. The CCD used is a Digital Pixel large format (maximum 1152 x 770 pixels) Peltier cooled (-20°C) device with a pixel size of 22.5 µm and a dynamic range of 4096. The apparatus is presented in schematic form in figure 1.

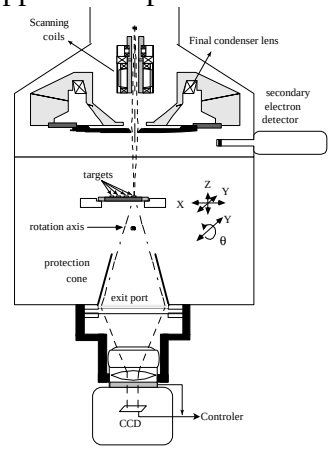

Figure 1 : Schematic representation of the microtomograph

The equivalent of the CCD pixel size on the phosphor screen is thus 22.5 x 1.6 = 36 µm. Resolution below this depends on the intrinsic magnification of the radiograph. Magnifications of over 100 are achievable reducing the equivalent detector element size to 0.36 µm. Such detector resolutions are seldom useful due to spatial resolution limitations induced by the electron beam size. However acquisition time can be greatly reduced by pixel

binning. In the results presented, 3 x 3 binning was used to obtain 256 x 256 images using 66 % of the active surface of the CCD whilst retaining the possibility of a one micron resolution limit of the detection system.

The two dimensional nature of the CCD detector means that microradiographs are produced directly without the need for beam or specimen displacement. For each specimen, a series of 120 (or 240) images (256 x 256 pixels) is recorded by rotating the specimen by 3° (or 1.5°) between successive micrographs. The reconstruction software, developed from that of Sasov [Sasov, 1987], uses the filtered back projection method and assumes parallel beam geometry which is a good approximation as long as the opening angle is less than 10°. The reconstruction time on a PC computer is of the order of one minute per section (256 x 256 pixels). The result is a 256 x 256 x 256 three dimensionnal microtomograph of the sample. Although in principle 400 angular steps are required to obtain a good reconstruction, it was found that 120 steps did not produce significant reconstruction artefacts whilst limiting the total acquistion time. Visualisation of volumic data is made via the Spyglass slicer software on PC. The surface of the reconstructed volume was compared when possible to surface images on a scanning electron microscope.

Results

Model and real porous media have been studied. Model porous media were created by filling 1 mm diameter borosilicate glass capillary tubes with silica glass beads of 30 to 200 µm diameter. Real porous media have been prepared from raw or resin embedded fragments of rocks, 1 to 2mm in diameter and 2 to 4 mm in length: a model reservoir rock, Fontainebleau sandstone, and three samples of a sandstone reservoir rock from the Brent formation of a North Sea Field (oil zone).

A niobium target (characteristic X-ray energy 16.6 keV) supported on carbon, excited by a 30 keV primary electron beam energy was used to obtain the radiographs.

Model porous media

A negative of a radiographic projection and a tomographic reconstruction of the model porous medium are shown in Plate I (Figure 2 to 4). An SEM image of a polished section of the sample is shown in Figure 5. The morphology of the glass beads is clearly reproduced although the resolution of the SEM is of course higher. The 3D visualisation software enables cropping the reconstructed object and extraction of a choosen volume of the sample. In this case, bubble type faults, 10 µm in diameter, clearly visible on both SEM images and the 3D reconstruction (arrows), attest to the resolution performance of the instrument (Fig 4).

Fontainebleau sandstone

Fontainebleau sandstone is a clay free sandstone currently used as a model reservoir rock. Plate II (Figure 6 to 14) shows the outer surface of the reconstructed tomograph (upper line) to be compared with SEM images of the same sample (middle line). Although the SEM images are of higher resolution, individual grains can clearly be seen in the tomographs. These images show the reliability of the reconstruction. Note that the epoxy glue used to fix the sample onto the rotation axis, clearly visible on the SEM images, is transparent to the X-rays used and does not hinder the visualisation of sub-surface grains.

Following images (lower line) are respectively, an SEM image of a polished section, the microtomograph from which a part has been extracted thus exposing three planes to be compared to the polished section, and finally, a part of the reconstructed porous network. The latter gives additional information about the pore connectivity.

Reservoir rocks

The studied samples come from a North Sea Field (Brent formation). Their mineralogical and petrophysical characteristics are reported in Table 1. These samples, although very similar in terms of petrophysical properties, have been shown [Durand, 1996] to exhibit different behavior in terms of wettability. The aim of this study was to compare the pore network of these rocks, to visualise the different mineralogical phases present in the rocks and to describe the 3D distribution of these phases, particularly feldspars and kaolinite. Cryo SEM experiments have shown a peculiar affinity of the latter for oil after ageing [Fassi, 1992, Durand, 1996].

	Units	CAR1	CAR3	CAR4
Porosity	%vol	15.9	16.6	22.6
Permeability	mD	50	340	560
Kaolinite	wt%	0	3.1	7.8
Illite	wt%	13.8	<1	.8
Quartz	wt%	83.7	92.5	67.4
K-Feldspars	wt%	0	3.3	16.8
Wettability		pref. oil wet	pref. water wet	pref. oil wet

Table 1 (from [Durand, 1996])

Pore networks

Each sample is described by a set of 250 slices (256 x 256 pixels). In these experiments, pixel size is not fixed but depends on the sample size. Pixel size are

respectively 8, 7 and 5.5 microns in the X, Y directions, and 11.5, 10.5, and 7.5 in the Z direction for CAR1, CAR3 and CAR4 samples.

Grey level histograms have been calculated from a set of 200 sections entirely included in the rock. They do not show well separated peaks and a deconvolution is necessary both to reach a semi-quantitative assessment of porosity or volume fraction of each phase and to make easier the choice of a threshold for phase separation. For this purpose, peaks were assumed to be gaussian and a fit was realized by minimizing square differences between model and data.

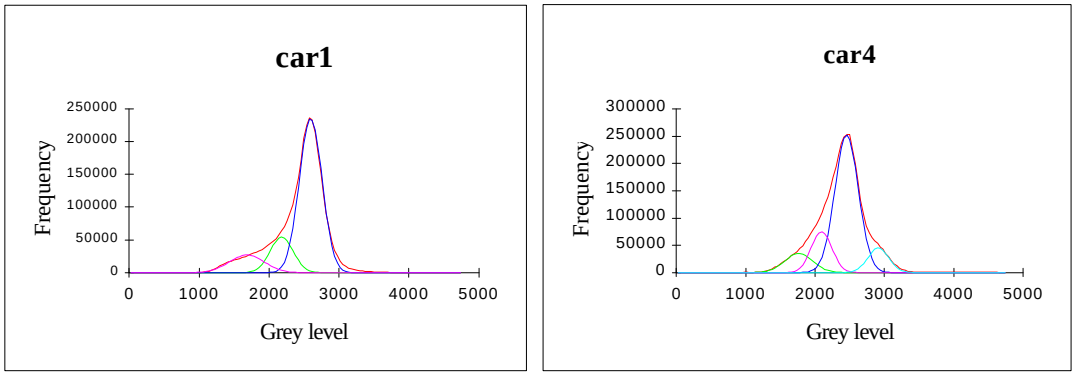

Figures 24 and 25: Grey level histograms of samples CAR1 and CAR4

Histograms can be described by the contribution of three peaks (four in the case of sample CAR4). The first corresponds to the pores the diameter of which is over the resolution limit. The second peak is a contribution of both pores under the resolution limit and loose clay agregates. Clays have the same absorption coefficient as quartz, a small size close to the resolution limit and are frequently associated with porosity. Therefore, they often appear with a grey level intermediate between the quartz grey level and the pore grey level. Compact agregates of clays with a size higher than the resolution cannot be distinguished from quartz by their grey level and are then classified in the central main peak, attributed to quartz. The fourth peak (in CAR4) can be identified as feldspars.

The % area of each peak has been measured for comparison with global measurements and results are reported in Table II._Global measurements give the total pore volume fraction while measurements from histograms give separately the fraction of macropores and the fraction of micropores plus clays. Comparison of the total volume fraction of pores plus clays shows good agreement between tomographic data and global analysis.

	CAR1		CAR3		CAR4	
Volume fraction	Global (%vol)	From hist (%vol).	Global (%vol)	From Hist (%vol)	Global (%vol)	From hist (%vol)
Pores >15 microns	16	13	17	11	22.6	10
Pores<15 microns		16		9		16
Clays	12		2.5		5	
Total:pores +clays	28	29	19.5	20	27.6	26
Quartz	71		77		62	
Feldspars	-		2.6	-	10.5	10

Table II: Volumic fraction of pores and minerals as deduced from global measurements [Durand, 1996] and measurements from grey level histograms.

For the CAR1 sample, nearly all of the porosity is accounted for by pores larger than 15 microns in diameter. Total porosity is 16% whilst large pores account for 13% of the rock volume. Only 20% of the pore volume is occupied by small pores. For CAR3 and particularly for CAR4, the volume occupied by the smaller pores is larger, one third for the sample CAR3 and one half for sample CAR4. Without information on the way these pores are connected, this trend would suggest an increasing permeability in the order CAR1>CAR3>CAR4 which is not the case. Observation of 3D reconstructions (Plate III, lower lines) gives an explanation to the opposite order found for the sample permeabilities.

Plate III gives for each of the three samples a SEM view of a polished section (upper line), a representation of the reconstructed volume of the samples (second line), and a representation of the macroporous network for two perpendicular orientations (lower lines). To enable the comparison of samples, the pore network has been represented in a fixed volume. The thresholds for pore network separation have been choosen from the histograms at the intersection between the first and the second peak in order to isolate macroporosity only. These thresholds are indicated on the corresponding pictures (Plate III, lower images). It appears that samples CAR3 and CAR4 have a comparable pore structure in which all macropores are well interconnected whilst CAR1 has much larger macropores but very few connections visible at this scale. The latter structure, combined with the relatively small micropore volume deduced from analysis of the histograms, explains the lower permeability.

Minerals

Feldpars

Feldspars are more absorbant than quartz and appear on reconstructions with a high grey level. Thus 3D distribution of feldspars in the rock can be easily described by segmentation [Ferreira De Paiva, 1995].

Kaolinite

Kaolinite identification and localisation is more delicate because its absorption coefficient is very near to the quartz and its size is critical (very near to the resolution limit) which makes its visualisation dependant on the way they are agregated (compact agregates, loose agregates, dispersed platelets). Compact agregates will appear with a grey level very near to quartz while loose agregates will appear with an intermediate grey level or, if the size of platelets is higher than 15 microns, as a very fine textured phase. These cases are illustrated for sample CAR4 on Plate IV (Figures 38 to 43). Figure 38 represents a part (900 x 800 µm) of the external surface of the reconstructed volume. An SEM image of the same area is presented on Figure 39, the EDS spectrum of kaolinite (a) being shown on Figure 40. Figure 41 to 43 are SEM magnified views of three parts of this area. In the first, kaolinite is agregated into packs 15 microns in diameter and about 15 µm apart. This zone is correctly reconstructed with a detail enabling the identification of kaolinite from its fine texture. On the second magnified view (Figure 42), kaolinite packs have the same size but their dispersion is less regular. Tightly assembled kaolinite appear as a massive phase with a texture and a grey level very similar to quartz, while dispersed kaolinites appear with a grey level very near to porosity. From this comparison, it appears that the resolution of the reconstruction is critical to distinguish kaolinite in all cases.

Discussion

Comparison of 3D porous networks in media of different permeability gives important information about the structure of the network, particularly concerning the accessibility of the pores which can be assessed by the pore/throat ratio. Sample CAR1 presents very large pores confined by small throats (below the resolution limit). From this pore structure, oil wettability of the rock CAR1 when compared to CAR3 may be explained in two ways:

1/ these fine throats impose a high capillary pressure for oil to penetrate into macropores and this pressure results in breaking of water films along the pore walls. Oil wettability of CAR1 would result in this case from a geometric effect.

2/ capillary pressure is not sufficient to break water films in either pore structure (sample CAR3 should be in this case more oil wet than CAR1) and the oil wet character of CAR1 would result from a mineralogical effect (presence of clays).

The information currently available does not allow us to fully eliminate one of these possibilities. Capillary pressure curves should allow us to conclude.

The mineralogical effect on wettability is more evident in the case of CAR3 and CAR4 which have opposite behaviors in terms of wettability and a very similar pore structure made of well interconnected macropores. The only difference between these two rocks is the presence of feldspars and kaolinite in CAR4. This is in agreement with Cryo SEM experiments which have shown a peculiar affinity of oil for altered feldpars and a modification of the wettability of kaolinite (from water wet to oil wet) under ageing in reservoir oil. One of the aims of this study was to examine whether the isolated 3D representation of feldspars + kaolinites would give a discontinuous or continuous

framework related to the wettability of the rock. In fact, although separation of feldspars is possible, the separation of kaolinite appears difficult due both to its small size, very close to resolution, and its absorption coefficient, comparable to that of quartz. Even an improved resolution of the order of a micron would not allow an exhaustive description of this mineral.

An improvement in resolution would be usefull to describe pore connectivity in low permeability media. A resolution of 2 microns has been reached on projections of glass samples [Ferreira De Paiva, 1996] and this can be considered as the actual resolution limit for this microtomograph. Nevertheless, the acquisition mode and number of projections imply a compromise between the resolution and the sample size. To reach 2 µm resolution implies working on very small volumes from which extrapolation to higher scales is difficult.

Samples studied here were 1 to 2 millimeters in diameter and 3 millimeters long. This appeared to be a good compromise between the required resolution and the representativity of the samples. In the case of heterogeneous samples, a number of representative samples per rock should be studied. This condition is not however limiting when laboratory equipment is available.

A contrast improvement would make the phase separation easier. Work is underway to achieve this by improving post acquisition and reconstruction treatments.

Conclusions

This laboratory microscanner allows in its standard uses a resolution of ten microns which already enables the study of some pore networks in reservoir rocks. The quality of reconstruction has been proved by comparing SEM images of the sample with the reconstructed surface of the sample. Both the qualitative impression from the 3D reconstructions and the quantitative data from grey level histograms suggest an explanation for the low permeability of the CAR1 sample. The porosity of this sample consists almost entirely of large isolated pores with little interconnection. This 3D connectivity description is not generally available from intrusion measurements of pore size distribution (which give information only on the pore throats) and may help assessing k/ϕ laws.

The limits on quantification of clay content are clear from these examples. Improving the spatial resolution will only push the problem to shorter length scales. Clays in closely packed aggregates cannot be distinguished from quartz, loosely packed clays are difficult to separate from porosity.

REFERENCES

CAZAUX J. THOMAS X., and MOUSE D. (1989) « Microscopie et Microtomographie X »
J. Microsc. Electronique, 14, p 263-276,1989

CHENG P.C., SHINOZAKID.M.,LIN T.H., NEWBURRY S.P., SRIDHAR R., TARNG W., CHEN M.T, CHEN L.H. (1992) « XRay Microscopy III» *edited by A. Michette et al. (Springer, Berlin, 1992)*

COLES M.E., SPANNE P., E.L. MUEGGE and K.W.JONES (1994) « Computed microtomography of reservoir core samples » *SCA Paper Number 9401 presented at 1994 Intern. Symp. of SCA, Stavenger, pages 9-16*

COLES M.E., HAZLETT R.D., SPANNE P. , SOLL W.E., MUEGGE E.L. , JONES K.W.(1996)
« Pore level imaging of fluid transport using synchrotron X-Ray Microtomography »
SCA Paper Number 9628 presented at 1996 Intern. Symp. of SCA, Montpellier , France

CUIEC L. (1991) « Evaluation of reservoir wettability and its effects on oil recovery »
Interfacial phenomena in petroleum recovery Ed. N. R. Morrow, Marcel Dekker Inc; , N.Y.

DURAND C. and ROSENBERG E. (1996) « Fluid distribution in kaolinite or illite-bearing cores. Cryo-SEM observations versus bulk measurements »
SCA Paper Number 9627 presented at 1996 Intern. Symp. of SCA, Montpellier , France

FASSI FIHRI O., ROBIN M. , and ROSENBERG E. (1992) « Etude de la mouillabilité des roches réservoirs à l'échelle du pore par Cryo Microscopie A Balayage » - Revue de l'IFP , VOL37,n°5,p. 685-701.

FERREIRA DE PAIVA R. (1995) « Developpement d'un microtomographe X et application à la caractérisation des roches réservoirs » *Thèse de Doctorat - Université Paris VI, France*

FERREIRA DE PAIVA R. , BISIAUX M., LYNCH J., ROSENBERG E.(1996) « High resolution X-Ray Tomography in an electron microprobe» *Rev. Sci. Instrum., 67 (6), June 1996*

SASOV A. Y. (1987) « Microtomography » *J. Microscopy*, 147,p169-178 et p 179-192

FIGURE NUMBERS ON PLATES I to IV

2	3
4	5

Plate I

6	7	8
9	10	11
12	13	14

Plate II

26	27	28
29	30	31
32	33	34
35	36	37

Plate III

38	39	40
41	42	43

Plate IV

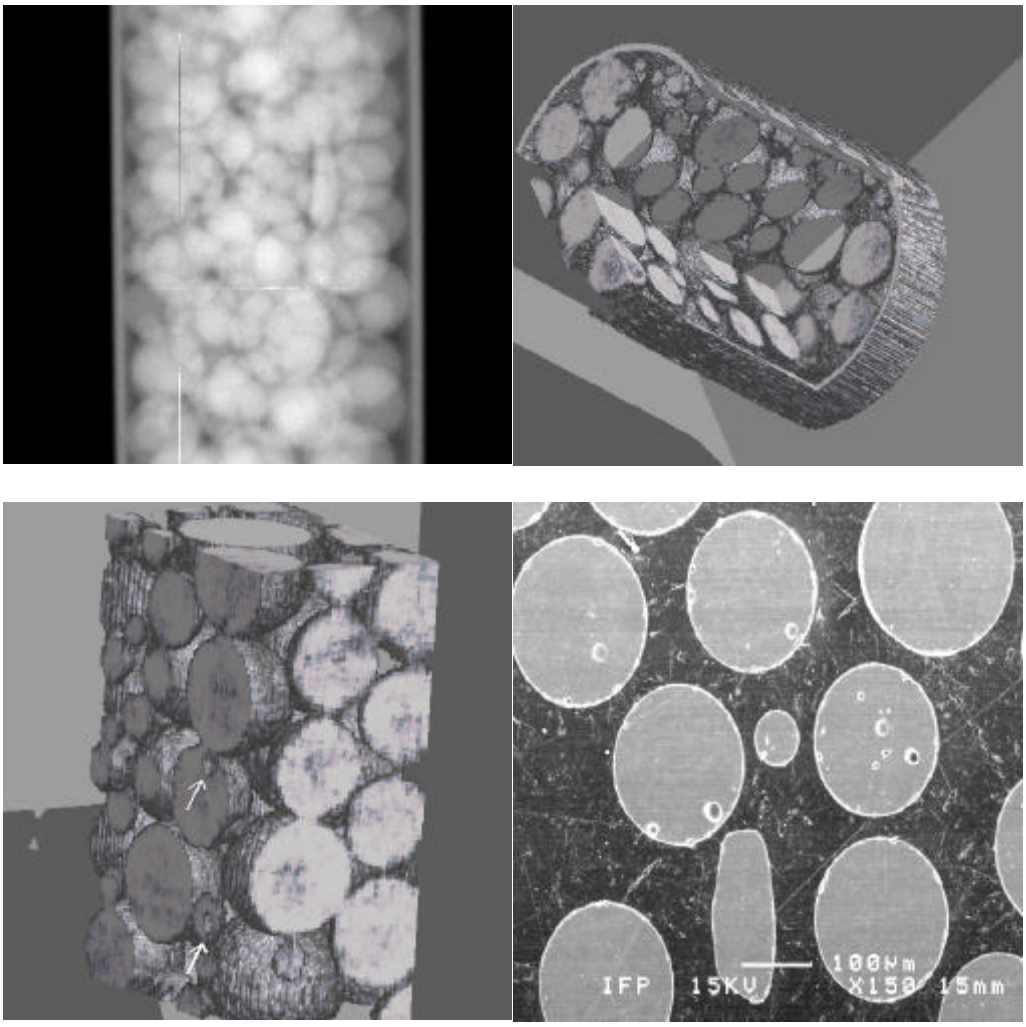

Plate I (Figures 2 to 5) : Model porous medium: glass beads in a capillary tube

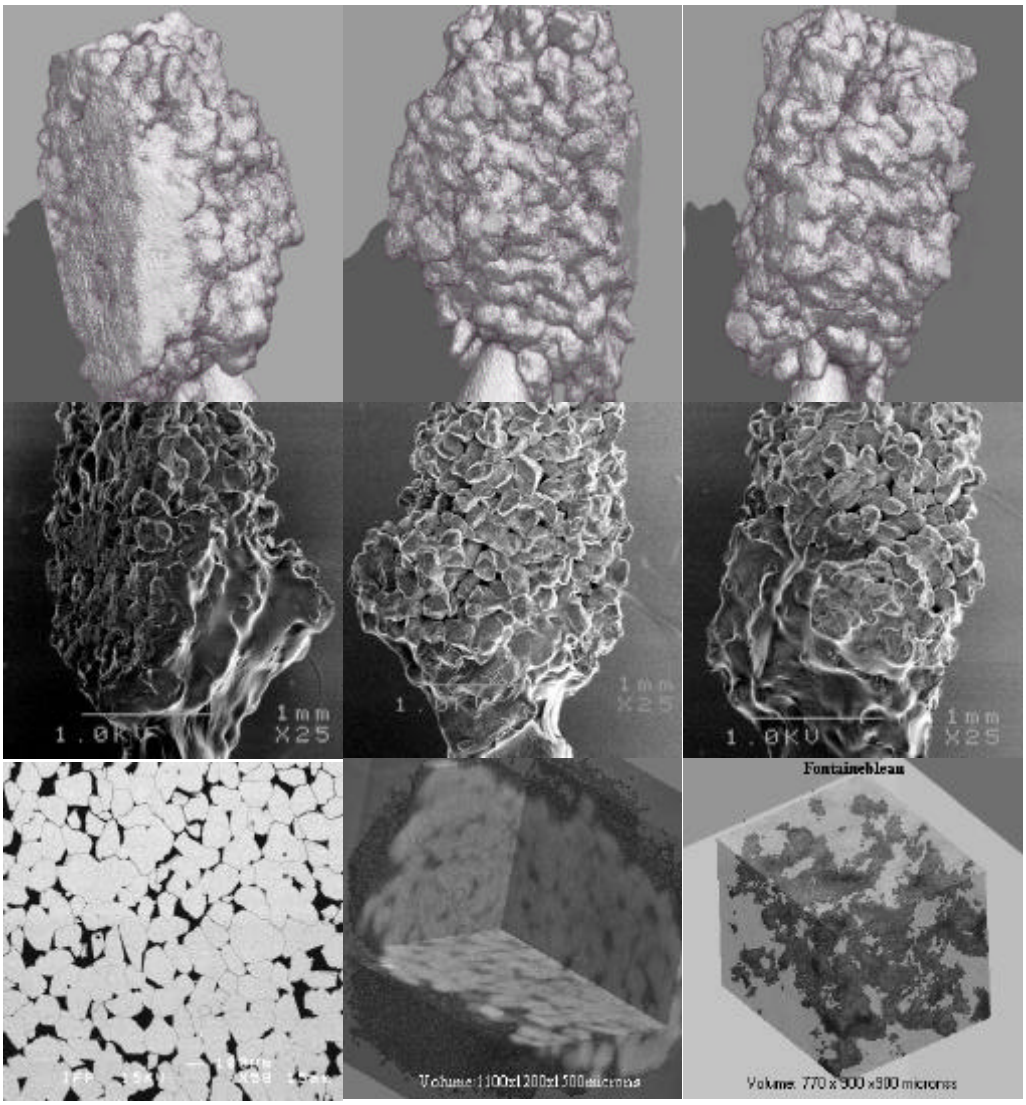

Plate II (Figures 6 to 14): Fontainebleau sandstone

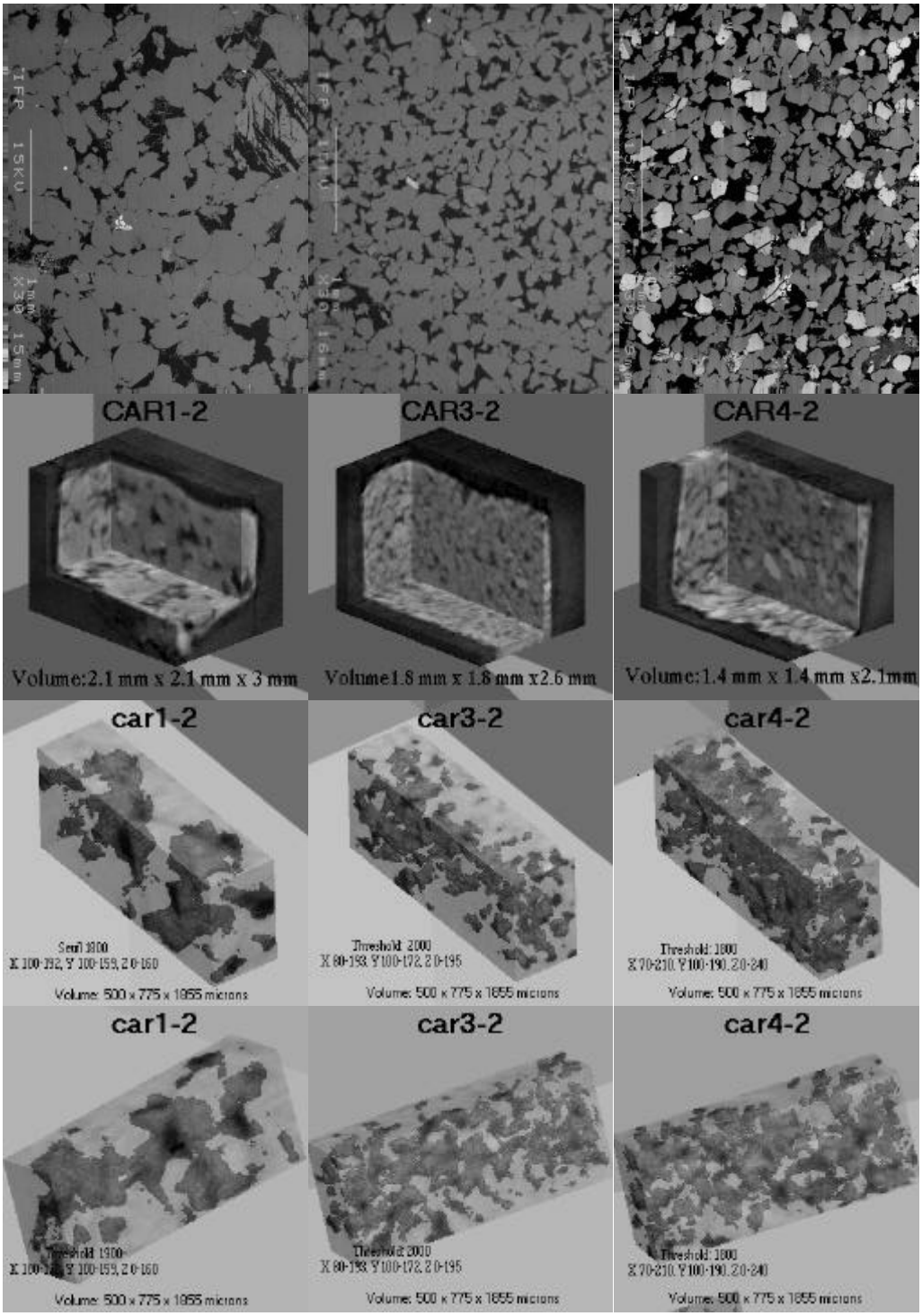

Plate III (Figures 26 to 37): SEM images (upper line) and Microtomograph reconstructions of three samples of reservoir rocks (respectively, CAR1, CAR3 and CAR4)

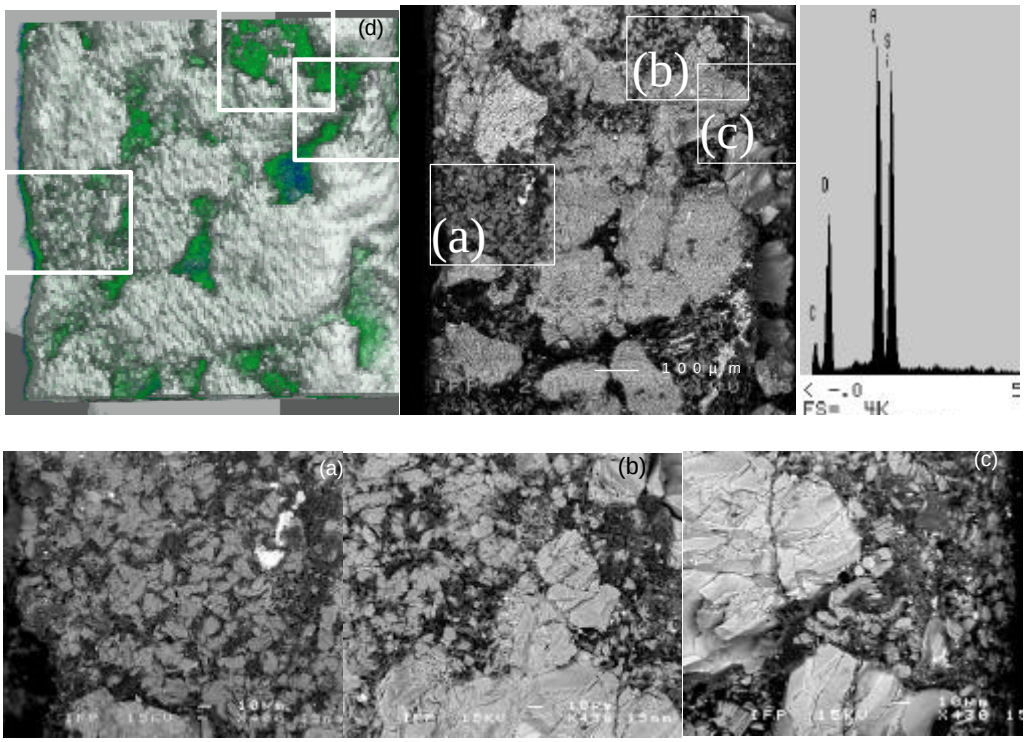

Plate IV (Figure 38 to 43): Comparison of SEM images and reconstructed surface in a zone rich in kaolinite (CAR4)